COBEM 2023 27TH INTERNATIONAL CONGRESS OF MECHANICAL ENGENEERING

ABCM Brazilian Society of Mechanical Sciences and Engineering
27th ABCM International Congress of Mechanical Engineering
December 04-08, 2023, Florianópolis-SC, Brazil

Convergence studies in elasticity with an independent basis isogeometric boundary element formulation

Guilherme Henrique Teixeira[1]
Francisco Alex Correira Monteiro[1]
Sergio Gustavo Ferreira Cordeiro[1]
[1]Aeronautics Institute of Technology, Laboratory of Structural Modelling, Praça Marechal Eduardo Gomes, 50, 12228-900. São José dos Campos-SP, Brazil.
guilhermeght@ita.br, facm@ita.br, cordeiro@ita.br

Abstract. *This work presents an independent basis isogeometric boundary element method (IGABEM). The geometry description is based on Non-Uniform Rational B-splines (NURBS) and independent B-splines basis are used for the unknown boundary fields. Lagrange polynomial basis are also applied for the boundary fields for comparative purposes. The boundary conditions are exactly considered and its contribution computed directly in the right-hand side vector of the linear system. This approach results a single-matrix formulation, improving storage requirements. The independence between geometry and boundary fields allows refinement strategies without changes in the geometry. Both knot insertion and k-refinement are applied for B-spline basis while p-refinement is applied for Lagrange polynomial basis. Convergence studied in terms of the L-2 norm of boundary fields are carried out in benchmark problems with available analytical solution. The results pointed-out that p-refined with equally spaced Lagrange polynomials suffers with the Runge Effect and diverges quickly. On the other hand, the p-refinement has convergence rates p+1 for b-splines basis of order p. As expected, the k- Refinement performed even better, with hypergeometric convergence. An open spanner problem is also presented for illustrative purposes.*

Keywords: *isogeometric analysis, boundary element method, independent basis, convergence studies*

1. INTRODUCTION

The numerical analysis of engineering problems requires the existence of geometric models. Even though Computer Aided Engineering (CAE) software allows direct model construction, the geometric design of complex engineering parts are usually developed in Computer-Aided Design (CAD) software, which are based on computational geometry concepts. The most common computational geometry technology adopted in CAD software are the Non-Uniform Rational B-spline (NURBS), which are built from NURBS basis functions (Piegl and Tiller, 1995). The main advantages of the NURBS are their ability to exact represent conics and quadrics as geometrical entities, such as cylinders, spheres and ellipsoids, and the fact that there are many efficient and stable algorithms for their computation (Cottrell *et al.*, 2009).

In the field of numerical analysis, the concept of Isogeometric Analysis (IGA) was introduced by Hughes *et al.* (2005) and Cottrell *et al.* (2006). The main goal of IGA is to integrate geometry and analysis models into a single model. To this end, basis functions adopted in CAD software (such as NURBS basis) are employed to the approximation of the unknown physical fields of boundary value problems. B-splines basis functions, the main technology in computational geometry, also posses very useful mathematical properties for numerical analysis. B-spline basis are a generalization of Bernstein polynomials, with excellent performance in analysis. They posses linear independence, point-wise positiveness, C_{p-1} continuity for a basis of order p and form a partition of unity. A new refinement strategy (k refinement) that results hypergeometric convergence in analysis is also an option with B-splines (Cottrell *et al.*, 2009). Due to such advantages, IGA were applied in several different types of numerical analysis (Cottrell *et al.*, 2006; Bazilevs *et al.*, 2009; Lipton *et al.*, 2010; Simpson *et al.*, 2012; Peng *et al.*, 2017; Beer and Duenser, 2023)

The boundary element method is a powerful method for solving boundary value problems when the differential equation that governs the physical problem is rewritten into boundary integral equations. The boundary integral equations can be obtained from integration by parts of a special weighted integral form of the differential equation, which uses fundamental solutions as weighting functions. The use of boundary integral equations can be traced back to Abel in 1823, who used them to solve the isochronous pendulum problem. Since then, many other works have been developed, as highlighted in a brief historical review provided by Hsiao (2006). Lachat and Watson (1976) were the first to use parametric boundary elements, where both the geometry and boundary fields are described by numerical approximation with basis functions. Two particular class of parametric boundary elements were studied by the authors: isoparametric boundary elements, in which basis functions of equal orders are employed for both geometry and boundary fields, and superparametric boundary boundary elements, in which the greater order is adopted for the boundary fields basis functions.

Isogeometric boundary elements can be understood as a particular case of isoparametric elements, if B-spline basis (or other computational geometry technology) are used for describing the geometrical boundary representation (B-rep)

and approximating the boundary fields. As refinement strategies in CAD does not change the parametric representation of the geometry, both isoparametric and superparametric concepts will produces an isogeometric formulation as long as B-spline basis are used for both geometry and fields approximation. Due to the fact the most CAD models are B-rep models, isogeometric boundary element methods (IGABEM) can provided a seamless integration between design and analysis (Marussig, 2015). Cervera and Trevelyan (2005) adopted NURBS curves in the geometry description in shape optimization boundary element analysis. Their approach however cannot be considered an isogeometric formulation, as they adopted conventional Lagrange polynomial basis functions for boundary displacement and traction fields. The idea of combining boundary element methods with Isogeometric Analysis (IGA) was first suggested by (Cottrell *et al.*, 2006). Since then, some works presented isogeometric boundary element formulations for different interesting applications, such as fracture mechanics, acoustic and electromagnetic scattering problems and underground excavations (Simpson *et al.*, 2012, 2014; Peng *et al.*, 2017; Liu *et al.*, 2017; Doz *et al.*, 2018; Beer and Duenser, 2023). A recent book about isogeometric boundary element methods can be found in (Beer *et al.*, 2020).

In contrast to using the isoparametric concept in isogeometric analysis, Marussig *et al.* (2015) describes an independent basis isogeometric boundary element formulation, in which refined higher order B-splines basis are adopted for the boundary fields, while keeping fixed the original NURBS basis provided by CAD for the boundary-representation geometry. The proposed approach violates the isoparametric concept. However, it is still isogeometric since the boundary fields B-splines basis are obtained from the refinement of the original CAD data, i.e. knot vectors and polynomial orders. The use of independent basis improves the flexibility for field refinement strategies. This is because independent basis allows the refinement of the boundary fields for a fixed geometry. The flexibility in refinement can be advantageous in practical applications, where the boundary fields may require different levels of refinement at specifically parts of the boundary, where the geometry can be described by simple lower order basis. Besides, the approach may be explored to improve the computational costs and storage memory requirements, as highlighted in Marussig *et al.* (2015).

The motivation for this work is to improve isogeometric boundary formulations by using NURBS geometric entities to represent the geometry and independent B-splines basis functions to approximate the unknown fields. Thus, refinement strategies can be applied without geometric changes. In addition, this work focuses one particular improvements: (i) imposing boundary conditions exactly into the boundary integral equations, resulting a single-matrix formulation that improves the memory storage requirements of the method, and (ii) using an auxiliar function in the displacement approximations to ensure boundary displacement continuity.

2. BASIS FUNCTIONS

Standard Lagrange polynomials and B-splines are chosen as basis functions for approximating the boundary fields. More extensive explanations about B-spline can be found in Beer *et al.* (2020).

2.1 Lagrange polynomials

Lagrange polynomials $L_p(\xi)$ are adopted for the interpolation of functions $f(\xi)$ in the form of

$$f(\xi) \approx L_p(\xi) = \sum_{i=1}^{p+1} L_{i,p}(\xi) f\left(\tilde{\xi}_i\right), \tag{1}$$

where $L_{i,p}(\xi)$ are Lagrange basis functions of order p, defined as

$$L_{i,p}(\xi) = \prod_{j=1, j\neq i}^{p+1} \frac{\xi - \tilde{\xi}_j}{\tilde{\xi}_i - \tilde{\xi}_j}, \quad j = 1, ..., p+1. \tag{2}$$

Approximations using Lagrange basis functions are commonly used in numerical analysis due to some important properties, such as the Kronecker delta property and the partition of unity. The Kronecker delta property, which ensures the interpolatory characteristic of the approximation, means that $L_{i,p}\left(\tilde{\xi}_j\right) = 1$ for $i = j$ and $L_{i,p}\left(\tilde{\xi}_j\right) = 0$ for $i \neq j$. In other words, $L_{i,p}\left(\tilde{\xi}_j\right) = \delta_{ij}$, with δ_{ij} being the Kronecker delta. The partition of unity property means that the sum of the basis function is always equal to one for any value of ξ.

2.2 B-splines

B-splines $B(\xi)$ are also an option for building approximations of functions $f(\xi)$ in the form of

$$f(\xi) \approx B(\xi) = \sum_{i=1}^{n} N_{i,p}(\xi) c_i, \tag{3}$$

where $N_{i,p}(\xi)$ are B-spline basis functions of order p and c_i are coefficients of the approximations. B-splines basis $N_{i,p}(\xi)$ are defined as piece-wise polynomial, which can be constructed from a non-decreasing set of coordinates

$$\Xi = \{\xi_1, \xi_2, ..., \xi_{n+p}, \xi_{n+p+1}\} \tag{4}$$

defined in the parameter space $\mathcal{P} = [\xi_i, \xi_{n+p+1}]$ of the B-spline, where p is the polynomial order and n the number of functions of the basis. The vector Ξ is denominated knot vector and consists of a total of $n + p + 1$ knots, which are the non-decreasing coordinates in $\mathcal{P}$. The interval between two consecutive knots $[\xi_i, \xi_{i+1}]$ is referred to as the knot span, which is usually mapped onto the Gaussian space for numerical integration purposes. B-spline basis functions can be constructed recursively. The recursive process starts with B-splines of order $p = 0$, which are piece-wise constant functions. For $p > 0$, B-spline bases can be obtained from the Cox–de Boor recursion formula (Cox, 1971; DeBoor, 1972)

$$N_{i,p} = \frac{\xi - \xi_i}{\xi_{i+p} - \xi_i} N_{i,p-1}(\xi) + \frac{\xi_{i+p+1} - \xi}{\xi_{i+p+1} - \xi_{i+1}} N_{i+1,p-1}(\xi). \tag{5}$$

For orders $p = 0$ and $p = 1$, the B-spline basis results the standard piece-wise constant and linear Lagrange basis. Quadratic or higher-order B-spline basis functions, however, differ from their Lagrange basis counterparts. B-splines exhibit some important properties for analysis, such as point-wise positiveness and local support, summarized as $N_{i,p}(\xi) > 0$ for $\xi \in [\xi_i, \xi_{i+p+1}]$ and $N_{i,p}(\xi) = 0$ otherwise. Moreover, a B-splines forms a partition of unit: $\sum_{i=1}^{n} N_{i,p}(\xi) = 1$.

The refinement of B-spline basis $N_{i,p}(\xi)$ can be done by modifying the initial knot vector Ξ and/or the polynomial order p, Aiming to increase the number of functions. This can be achieved through various techniques such as order elevation, knot insertion, or k-refinement. All this techniques can be found in Hughes *et al.* (2005).

2.3 NURBS curves

NURBS curves in a $\mathcal{R}^d$ space, defined by piecewise rational basis functions, are obtained by the projection of B-spline curves in $\mathcal{R}^{d+1}$. For instance, NURBS curves in $\mathcal{R}^2$ are obtained from projective transformations of B-splines curves in $\mathcal{R}^3$.

The B-splines basis functions, given in Eq. (5), can be used to describe a B-spline curve in the $\mathcal{R}^3$ space. This curve is defined as a linear combination of the basis functions $N_{i,p}(\xi)$, where $i = 1, 2, ..., n$, and the control points $\mathbf{C}_i \in \mathcal{R}^3$

$$\mathbf{c}(\xi) = \sum_{i=1}^{n} N_{i,p}(\xi)\mathbf{C}_i. \tag{6}$$

Defining weights w_i as the z-components of the of control points c, it is possible obtain a NURBS curve in $\mathcal{R}^2$

$$\mathbf{x}(\xi) = \sum_{i=1}^{n} R_{i,p}(\xi)\mathcal{B}_i, \tag{7}$$

in which the NURBS basis functions are defined as

$$R_{i,p}(\xi) = \frac{N_{i,p}(\xi)w_i}{\sum_{j=1}^{n} N_{j,p}(\xi)w_j}. \tag{8}$$

The control points $\mathcal{B}_i$ of the NURBS curves are defined by the x- and y-components of the B-spline control points $\mathbf{C}_i$. The control points are points $\rfloor_i$ and $\mathcal{B}_i$ in the physical space $\mathcal{R}^d$, $d = 3$ or $d = 2$, where the B-spline and NURBS curves are defined.

3. INDEPENDENT BASIS IGABEM FORMULATION

3.1 Boundary discretization

The vector-valued problem of linear elasticity expressed in terms of boundary integral equation is used to exemplify the independent basis IGABEM formulation. The boundary S of the domain of a given elasticity problem may be decomposed into complementary Neumann and Dirichlet parts for each direction: $S = S_{u_x} \cup S_{t_x}$, with $S_{u_x} \cap S_{t_x} = \emptyset$, or $S = S_{u_y} \cup S_{t_y}$, with $S_{u_y} \cap S_{t_y} = \emptyset$. At a boundary S_{u_l}, $l = x, y$, the displacement $\overline{u}_l(\mathbf{x})$ is prescribed and the traction field $t_l(\mathbf{x})$ is unknown, while at a boundary S_{t_l}, $l = x, y$, the traction $\overline{t}_l(\mathbf{x})$ is prescribed and the displacement field $u_l(\mathbf{x})$ is unknown. The boundaries S_{u_l} and S_{t_l} are discretized into small parts called elements, where geometry parametrization by NURBS curves and boundary fields approximation are employed. Therefore: $S_{u_l} = \bigcup_{e=1}^{N_{ul}} S^e_{u_l}$ and $S_{t_l} = \bigcup_{e=1}^{N_{tl}} S^e_{t_l}$.

The displacement field $u^e_l(\mathbf{x})$ is unknown in all elements of the type S^e_t, where the traction field $\overline{t}^e_l(\mathbf{x})$ is prescribed. Similarly, the field $t^e_l(\mathbf{x})$ is unknown in all elements of type S^e_u, where $\overline{u}^e_l(\mathbf{x})$ is prescribed. In the present work, only the

unknown fields are approximated by basis functions, which are not the NURBS basis adopted for geometry parametrization. Given two arbitrary set of linearly independent functions $\{N_j^e\}_{j=1}^{n_e}$ and $\{M_j^e\}_{j=1}^{m_e}$, it is possible to propose the following approximations

$$\tilde{u}_l^e(\mathbf{x}) = u_{0l}^e(\mathbf{x}) + N_j^e u_{lj}^e \qquad \forall \mathbf{x} \in S_{t_l}^e \qquad l = x, y \tag{9}$$

$$\tilde{t}_l^e(\mathbf{x}) = M_j^e(\mathbf{x})\, q_{lj}^e \qquad \forall \mathbf{x} \in S_{u_l}^e \qquad l = x, y \tag{10}$$

where $u_{0l}^e(\mathbf{x})$ is an auxiliary function used to ensure continuity between prescribed and non-prescribed boundary displacements. The basis $\{N_j^e\}_{j=1}^{n_e}$ and the functions $u_{0l}^e(\mathbf{x})$ must satisfy

$$u_{0l}^e(\mathbf{x}_b) = \overline{u}_l(\mathbf{x}_b) \text{ and } N_j^e(\mathbf{x}_b) = 0 \quad \text{at points } \mathbf{x}_b \in \partial S_{u_l}^e \cap \partial S_{t_l}^e \tag{11}$$

in order to ensure the continuity between approximations and the prescribed boundary conditions at boundary points $\mathbf{x}_b \in \partial S_{u_l}^e \cap \partial S_{t_l}^e$, which connects boundaries S_{u_l} and S_{t_l}. A basis $\{B_j\}_{j=1}^{q}$ that satisfy the Kronecker Delta property at the ends of the element, in other words, a basis which is interpolatory at the end-points $\mathbf{x}(\xi_1)$ and $\mathbf{x}(\xi_q)$ of an element $S_{t_l}^e$, such as the one illustrated in Fig. 1 , allows to define the function u_{0l}^e and the basis $\{N_j^e\}_{j=1}^{n_e}$.

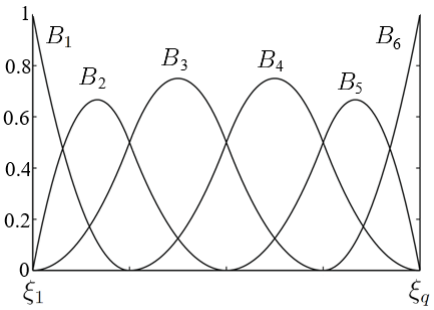

Figure 1. Basis $\{B_j\}_{j=1}^{6}$ with interpolatory at the end points

There are four different possibilities for elements of the type $S_{t_l}^e$: (i) elements that not intercept a boundary $S_{u_l}^e$, (ii) elements that intercept a boundary $S_{u_l}^e$ at $\mathbf{x}(\xi_1)$, (iii) elements that intercept a boundary $S_{u_l}^e$ at $\mathbf{x}(\xi_q)$, and (iv) elements that intercept boundaries $S_{u_l}^e$ at $\mathbf{x}(\xi_1)$ and $\mathbf{x}(\xi_q)$. These four different elements result in different definitions for $u_{0l}^e(\mathbf{x})$ and $\{N_{j^e}\}_{j=1}^{n_e}$

$$u_{0l}^e(\mathbf{x}(\xi)) = 0 \qquad \text{and} \quad \left\{N_j^e\right\}_{j=1}^{n_e=q} = \{B_j\}_{j=1}^{q} \qquad \text{for case (i)} \tag{12}$$

$$u_{0l}^e(\mathbf{x}(\xi)) = u_{0_1} B_1(\xi) \qquad \text{and} \quad \left\{N_j^e\right\}_{j=1}^{n_e=q-1} = \{B_j\}_{j=2}^{q} \quad \text{for case (ii)} \tag{13}$$

$$u_{0l}^e(\mathbf{x}(\xi)) = u_{0_q} B_q(\xi) \qquad \text{and} \quad \left\{N_j^e\right\}_{j=1}^{n_e=q-1} = \{B_j\}_{j=1}^{q-1} \quad \text{for case (iii)} \tag{14}$$

$$u_{0l}^e(\mathbf{x}(\xi)) = u_{0_1} B_1(\xi) + u_{0_q} B_q(\xi) \quad \text{and} \quad \left\{N_j^e\right\}_{j=1}^{n_e=q-2} = \{B_j\}_{j=2}^{q-1} \quad \text{for case (iv)} \tag{15}$$

where $u_{0_1} = \overline{u}_l(\mathbf{x}_1)$ and $u_{0_q} = \overline{u}_l(\mathbf{x}_q)$ are prescribed the values of u_l at $\mathbf{x}_1$ and $\mathbf{x}_q$. Continuity is not imposed for the approximation $\tilde{t}_l^e(\mathbf{x})$ because the field t_l is discontinuous by nature. Lagrange polynomial and B-splines basis can be employed as basis $\{B_j\}_{j=1}^{q}$. For boundary value problems with $S_{u_x} = S_{u_y} = S_u$ and, consequently $S_{t_x} = S_{t_y} = S_t$, approximations using the definitions in Equations (13), (14) and (15) can be applied to ensure the continuity of the displacement boundary field. Otherwise, Equation (12) must be considered for all types of elements $S_{t_l}^e$ and displacement continuity is lost. In the following, $S_{u_x} = S_{u_y} = S_u$, $S_{t_x} = S_{t_y} = S_t$ is considered.

3.2 Collocation of boundary integral equations

The displacement boundary integral equation (BIE) of Navier-Cauchy elasticity equations can be written as

$$0 = c_{kl}(\mathbf{x}_0)\, u_l(\mathbf{x}_0) + \mathcal{C} \int_{S_u} t_{kl}^* u_l \, dS + \int_{S_t} t_{kl}^* u_l \, dS - \int_{S_u} u_{kl}^* t_l \, dS - \int_{S_t} u_{kl}^* t_l \, dS \tag{16}$$

for $\mathbf{x}_0 \in S_u = S_{u_x} = S_{u_y}$ and as

$$0 = c_{kl}(\mathbf{x}_0)\, u_l(\mathbf{x}_0) + \int_{S_u} t_{kl}^* u_l \, dS + \mathcal{C} \int_{S_t} t_{kl}^* u_l \, dS - \int_{S_u} u_{kl}^* t_l \, dS - \int_{S_t} u_{kl}^* t_l \, dS \tag{17}$$

for $\mathbf{x}_0 \in S_t = S_{t_x} = S_{t_y}$. The displacements and tractions components are denoted by $u_l(\mathbf{x})$ and $t_l(\mathbf{x})$, respectively. The source point $\mathbf{x}_0$ and the fields point $\mathbf{x}$ are located at the boundary S, with normal outward vector $\mathbf{n}$. The terms $u^*_{kl}(\mathbf{x}, \mathbf{x}_0)$ and $t^*_{kl}(\mathbf{x}, \mathbf{x}_0)$ are the Kelvin fundamental solution for plane linear elasticity (Beer *et al.*, 2020). The term $c(\mathbf{x}_0)\, u_k(\mathbf{x}_0)$ is a free term resulted from the singular integrals.

The boundary S_u and S_t are discretizated, respectively, into N_u and N_t parts: $S_u = \bigcup_{e=1}^{N_u} S_u^e$ and $S_t = \bigcup_{e=1}^{N_t} S_t^e$. The introduction of the boundary discretization and the definition of the approximations Eq. (9) and Eq. (10) over S_t^e and S_u^e leads to the residues

$$r_k^u(\mathbf{x}_0) = c(\mathbf{x}_0)\, \overline{u}_k^{e_0}(\mathbf{x}_0) + \sum_{e=1}^{N_u} \int_{S_u^e} t^*_{kl}(\mathbf{x}^e, \mathbf{x}_0)\, \overline{u}_l^e(\mathbf{x}^e)\, dS + \sum_{e=1}^{N_t} \int_{S_t^e} t^*_{kl}(\mathbf{x}^e, \mathbf{x}_0)\, \tilde{u}_l^e(\mathbf{x}^e)\, dS \tag{18}$$

$$- \sum_{e=1}^{N_u} \int_{S_u^e} u^*_{kl}(\mathbf{x}^e, \mathbf{x}_0)\, \tilde{t}_l^e(\mathbf{x}^e)\, dS - \sum_{e=1}^{N_t} \int_{S_t^e} u^*_{kl}(\mathbf{x}^e, \mathbf{x}_0)\, \overline{t}_l^e(\mathbf{x}^e)\, dS$$

for $\mathbf{x}_0 \in S_u^{e_0}$ and as

$$r_k^t(\mathbf{x}_0) = c(\mathbf{x}_0)\, \tilde{u}_k^{e_0}(\mathbf{x}_0) + \sum_{e=1}^{N_u} \int_{S_u^e} t^*_{kl}(\mathbf{x}^e, \mathbf{x}_0)\, \overline{u}_l^e(\mathbf{x}^e)\, dS + \sum_{e=1}^{N_t} \int_{S_t^e} t^*_{kl}(\mathbf{x}^e, \mathbf{x}_0)\, \tilde{u}_l^e(\mathbf{x}^e)\, dS \tag{19}$$

$$- \sum_{e=1}^{N_u} \int_{S_u^e} u^*_{kl}(\mathbf{x}^e, \mathbf{x}_0)\, \tilde{t}_l^e(\mathbf{x}^e)\, dS - \sum_{e=1}^{N_t} \int_{S_t^e} u^*_{kl}(\mathbf{x}^e, \mathbf{x}_0)\, \overline{t}_l^e(\mathbf{x}^e)\, dS$$

for $\mathbf{x}_0 \in S_t^{e_0}$. Note that different residues are defined depending on the position of the source point. The first index $(k = x, y)$ is related to the direction of the punctial force in the fundamental problem, while the second index $(l = x, y)$ is related to the response directions in the real problem.

The geometrical parametrizations $\mathbf{x}^e(\xi)$ are based on NURBS curves

$$\mathbf{x}^e(\xi) = \sum_{i=1}^{n} R^e_{i,p}(\xi) \mathbf{B}^e_i, \tag{20}$$

where $R^e_{i,p}(\xi)$ and $\mathbf{B}^e_i$ are the basis functions and the control points of the curves $\mathbf{x}^e(\xi)$, which are parametrizations of S_u^e or S_t^e. The integrals in Eq. (18) and Eq. (19) becomes improper when the source point $\mathbf{x}_0$ is located on the element to be integrated. With the introduction of the approximations, the residues $r_k^u(\mathbf{x}_0)$ and $r_k^t(\mathbf{x}_0)$ are not necessarily null for a general source point $\mathbf{x}_0$. The collocation weighted residual method is employed to obtain the degrees of freedom of the approximations. For collocation points $\mathbf{x}_i \in S_u$, the associated weight functions are $w_i^u = \delta(||\mathbf{x}_0 - \mathbf{x}_i||)$, with $i = 1, ..., M$. Similarly, for collocation points $\mathbf{x}_i \in S_t$, the associated weight functions are $w_i^t = \delta(||\mathbf{x}_0 - \mathbf{x}_i||)$, with $i = M+1, ..., M+N$. N and M correspond to the global number of unknowns values u^e_{lj} and t^e_{lj}, respectively. The weights $\delta(||\mathbf{x}_0 - \mathbf{x}_i||)$ are Dirac delta centered on $\mathbf{x}_i \in S_u$ or $\mathbf{x}_i \in S_t$. The collocation method results

$$\left\{ \begin{array}{c} \langle r_k^u, w_i^u \rangle \\ \langle r_k^t, w_i^t \rangle \end{array} \right\} = \left\{ \begin{array}{c} (0_k)_i \\ (0_k)_i \end{array} \right\} \Rightarrow \left\{ \begin{array}{c} r_k^u(\mathbf{x}_i) \\ r_k^t(\mathbf{x}_i) \end{array} \right\} = \left\{ \begin{array}{c} (0_k)_i \\ (0_k)_i \end{array} \right\} \tag{21}$$

or

$$\left\{ \begin{array}{c} \mathbf{f}_k^u \\ \mathbf{f}_k^t \end{array} \right\} + \left\{ \begin{array}{c} \mathbf{m}_k^u \\ \mathbf{m}_k^t \end{array} \right\} = \left\{ \begin{array}{c} \mathbf{0}_k \\ \mathbf{0}_k \end{array} \right\} \tag{22}$$

in which the components $(f_k^u)_i$, $(f_k^t)_i$, $(m_k^u)_i$ and $(m_k^t)_i$ can be expressed as

$$(f_k^u)_i = c(\mathbf{x}_i)\, \overline{u}_k^{e_i}(\mathbf{x}_i) + (f_{kx})_i + (f_{ky})_i \tag{23}$$

$$\left(f_k^t\right)_i = c(\mathbf{x}_i)\, u_{0k}^{e_i}(\mathbf{x}_i) + (f_{kx})_i + (f_{ky})_i \tag{24}$$

$$(m_k^u)_i = (m_{kx})_i + (m_{ky})_i \tag{25}$$

$$\left(m_k^t\right)_i = c(\mathbf{x}_i)\, N_j^{e_i}(\mathbf{x}_i)\, u_{kj}^{e_i} + (m_{kx})_i + (m_{ky})_i. \tag{26}$$

Note that e_i is the number of the element $S_u^{e_i}$ or $S_t^{e_i}$ which contains $\mathbf{x}_i$. The collocations points over the boundaries $S_u^{e_i}$ are chosen as the mapping $\mathbf{x}(\xi_i)$ evaluated at the anchor points ξ_i of the basis $\left\{M_j^e\right\}_{j=1}^{m_e}$, while the collocations points

over the boundaries $S_t^{e_i}$ are chosen as the mapping $\mathbf{x}(\xi_i)$ evaluated at the anchor points ξ_i of the basis $\left\{N_j^e\right\}_{j=1}^{n_e}$. The contributions $(f_{kx})_i$ and $(f_{ky})_i$ in Equations (23) and (24) are defined as

$$(f_{kx})_i = \sum_{e=1}^{N_u} \int_{S_u^e} t_{kx}^*\left(\mathbf{x}^e, \mathbf{x}_i\right) \overline{u}_x^e\left(\mathbf{x}^e\right)\, dS + \sum_{e=1}^{N_t} \int_{S_t^e} t_{kx}^*\left(\mathbf{x}^e, \mathbf{x}_i\right) u_{0x}^e\left(\mathbf{x}^e\right)\, dS - \sum_{e=1}^{N_t} \int_{S_t^e} u_{kx}^*\left(\mathbf{x}^e, \mathbf{x}_i\right) \overline{t}_x^e\left(\mathbf{x}^e\right)\, dS \quad (27)$$

$$(f_{ky})_i = \sum_{e=1}^{N_u} \int_{S_u^e} t_{ky}^*\left(\mathbf{x}^e, \mathbf{x}_i\right) \overline{u}_y^e\left(\mathbf{x}^e\right)\, dS + \sum_{e=1}^{N_t} \int_{S_t^e} t_{ky}^*\left(\mathbf{x}^e, \mathbf{x}_i\right) u_{0y}^e\left(\mathbf{x}^e\right)\, dS - \sum_{e=1}^{N_t} \int_{S_t^e} u_{ky}^*\left(\mathbf{x}^e, \mathbf{x}_i\right) \overline{t}_y^e\left(\mathbf{x}^e\right)\, dS \quad (28)$$

and can be directly computed once the auxilar functions $u_{0l}^e(\xi)$ and the exact boundary conditions $\overline{u}_l^e$, $\overline{t}_l^e$ are properly defined over the boundaries S_u^e and S_t^e. On the other hand, the components $(m_{kx})_i$ and $(m_{ky})_i$, which are defined as

$$(m_{kx})_i = \sum_{e=1}^{N_t} \int_{S_t^e} t_{kx}^*\left(\mathbf{x}^e, \mathbf{x}_i\right) N_j^e\left(\mathbf{x}^e\right)\, dS\ \ u_{xj}^e\ - \sum_{e=1}^{N_u} \int_{S_u^e} u_{kx}^*\left(\mathbf{x}^e, \mathbf{x}_i\right) M_j^e\left(\mathbf{x}^e\right)\, dS\ \ t_{xj}^e \quad (29)$$

$$(m_{ky})_i = \sum_{e=1}^{N_t} \int_{S_t^e} t_{ky}^*\left(\mathbf{x}^e, \mathbf{x}_i\right) N_j^e\left(\mathbf{x}^e\right)\, dS\ \ u_{yj}^e\ - \sum_{e=1}^{N_u} \int_{S_u^e} u_{ky}^*\left(\mathbf{x}^e, \mathbf{x}_i\right) M_j^e\left(\mathbf{x}^e\right)\, dS\ \ t_{yj}^e \quad (30)$$

cannot be directly computed because the coefficients u_{xj}^e, u_{yj}^e, t_{xj}^e, t_{yj}^e are not known a priory. However, the components $(m_k^u)_i$ and $(m_k^t)_i$ defined in Equations (25) and Eq. (26) can be rewritten as

$$(m_k^u)_i = \sum_{e=1}^{N_t} (H_{kx})_{ij}^{u_e}\, u_{xj}^e + \sum_{e=1}^{N_t} (H_{ky})_{ij}^{u_e}\, u_{yj}^e - \sum_{e=1}^{N_u} (G_{kx})_{ij}^{u_e}\, t_{xj}^e - \sum_{e=1}^{N_u} (G_{ky})_{ij}^{u_e}\, t_{yj}^e \quad (31)$$

$$\left(m_k^t\right)_i = c_{kx}\left(\mathbf{x}_i\right) N_j^{e_i}\left(\mathbf{x}_i\right) u_{xj}^{e_i} + \sum_{e=1}^{N_t} (\hat{H_{kx}})_{ij}^{t_e} u_{xj}^e + c_{ky}\left(\mathbf{x}_i\right) N_j^{e_i}\left(\mathbf{x}_i\right) u_{yj}^{e_i} + \sum_{e=1}^{N_t} (\hat{H_{ky}})_{ij}^{t_e} u_{yj}^e \quad (32)$$

$$- \sum_{e=1}^{N_u} (G_{kx})_{ij}^{t_e}\, t_{xj}^e - \sum_{e=1}^{N_u} (G_{ky})_{ij}^{t_e}\, t_{yj}^e$$

in which

$$(H_{kl})_{ij}^{u_e} = \int_{S_t^e} t_{kl}^*\left(\mathbf{x}^e, \mathbf{x}_i\right) N_j^e\left(\mathbf{x}^e\right)\, dS \qquad \forall \mathbf{x}_i \in \mathrm{S}_u^e \quad (33)$$

$$(G_{kl})_{ij}^{u_e} = \int_{S_u^e} u_{kl}^*\left(\mathbf{x}^e, \mathbf{x}_i\right) M_j^e\left(\mathbf{x}^e\right)\, dS \qquad \forall \mathbf{x}_i \in \mathrm{S}_u^e \quad (34)$$

$$(\hat{H_{kl}})_{ij}^{u_e} = \int_{S_t^e} t_{kl}^*\left(\mathbf{x}^e, \mathbf{x}_i\right) N_j^e\left(\mathbf{x}^e\right)\, dS \qquad \forall \mathbf{x}_i \in \mathrm{S}_t^e \quad (35)$$

$$(G_{kl})_{ij}^{t_e} = \int_{S_u^e} u_{kl}^*\left(\mathbf{x}^e, \mathbf{x}_i\right) M_j^e\left(\mathbf{x}^e\right)\, dS \qquad \forall \mathbf{x}_i \in \mathrm{S}_t^e. \quad (36)$$

The integrals in Equations (27)-(28) and (33)-(36) can be computed with standard Gauss-Legendre quadrature when the collocation point $\mathbf{x}_i$ does not lay on the element to be integrated. When $\mathbf{x}_i$ belongs to the element of integration, the integrals become improper and the subtraction singularity regularization must be applied (Aliabadi, 2002).

Defining

$$(H_{kx})_{ij}^{t_e} = c_{kx}\left(\mathbf{x}_i\right) N_j^{e_i}\left(\mathbf{x}_i\right) + (\hat{H_{kx}})_{ij}^{t_e} \quad \text{for} \quad e = e_i \quad (37)$$

$$(H_{kx})_{ij}^{t_e} = (\hat{H_{kx}})_{ij}^{t_e} \quad \text{for} \quad e \neq e_i \quad (38)$$

and

$$(H_{ky})_{ij}^{t_e} = c_{ky}\left(\mathbf{x}_i\right) N_j^{e_i}\left(\mathbf{x}_i\right) + (\hat{H_{ky}})_{ij}^{t_e} \quad \text{for} \quad e = e_i \quad (39)$$

$$(H_{ky})_{ij}^{t_e} = (\hat{H_{ky}})_{ij}^{t_e} \quad \text{for} \quad e \neq e_i, \quad (40)$$

Equations (31) and (32) can be rewritten as

$$(m_k^u)_i = \sum_{e=1}^{N_t} (H_{kx})_{ij}^{u_e}\, u_{xj}^e + \sum_{e=1}^{N_t} (H_{ky})_{ij}^{u_e}\, u_{yj}^e - \sum_{e=1}^{N_u} (G_{kx})_{ij}^{u_e}\, t_{xj}^e - \sum_{e=1}^{N_u} (G_{ky})_{ij}^{u_e}\, t_{yj}^e \tag{41}$$

$$\left(m_k^t\right)_i = \sum_{e=1}^{N_t} (H_{kx})_{ij}^{t_e}\, u_{xj}^e + \sum_{e=1}^{N_t} (H_{ky})_{ij}^{t_e}\, u_{yj}^e - \sum_{e=1}^{N_u} (G_{kx})_{ij}^{t_e}\, t_{xj}^e - \sum_{e=1}^{N_u} (G_{ky})_{ij}^{t_e}\, t_{yj}^e \tag{42}$$

and expressed in matrix formt as

$$\mathbf{m}_k^u = \sum_{e=1}^{N_t} \mathbf{H}_{kx}^{u_e}\mathbf{u}_x^e + \sum_{e=1}^{N_t} \mathbf{H}_{ky}^{u_e}\mathbf{u}_y^e - \sum_{e=1}^{N_u} \mathbf{G}_{kx}^{u_e}\mathbf{t}_x^e - \sum_{e=1}^{N_u} \mathbf{G}_{ky}^{u_e}\mathbf{t}_y^e \tag{43}$$

$$\mathbf{m}_k^t = \sum_{e=1}^{N_t} \mathbf{H}_{kx}^{t_e}\mathbf{u}_x^e + \sum_{e=1}^{N_t} \mathbf{H}_{ky}^{t_e}\mathbf{u}_y^e - \sum_{e=1}^{N_u} \mathbf{G}_{kx}^{t_e}\mathbf{t}_x^e - \sum_{e=1}^{N_u} \mathbf{G}_{ky}^{t_e}\mathbf{t}_y^e. \tag{44}$$

Regarding the connectivity of the equally classified boundaries S_u^e or S_t^e, equations (43) and (44) results

$$\mathbf{m}_k^u = \mathbf{H}_{kx}^u\mathbf{u}_x + \mathbf{H}_{ky}^u\mathbf{u}_y - \mathbf{G}_{kx}^u\mathbf{t}_x - \mathbf{G}_{ky}^u\mathbf{t}_y \tag{45}$$

$$\mathbf{m}_k^t = \mathbf{H}_{kx}^t\mathbf{u}_x + \mathbf{H}_{ky}^t\mathbf{u}_y - \mathbf{G}_{kx}^t\mathbf{t}_x - \mathbf{G}_{ky}^t\mathbf{t}_y \tag{46}$$

in which the vectors $\mathbf{u}_l$ and $\mathbf{t}_l$ collect, respectively, all the N boundary values u_{lj} and all the M boundary values t_{lj}. The global matrices $\mathbf{H}_{kl}^u$, $\mathbf{G}_{kl}^u$, $\mathbf{H}_{kl}^t$ and $\mathbf{G}_{kl}^t$ are, respectively, $M \times N$, $M \times M$, $N \times N$, $N \times M$ matrices in which the rows are associated with the number of collocation points, related to the corresponding residue, and the columns associated with the number of basis functions.

Regarding equations (22), (45) and (46), the final boundary element collocation system results

$$\mathbf{A}\mathbf{x} = -\mathbf{f}, \tag{47}$$

in which

$$\mathbf{A} = \begin{bmatrix} \mathbf{H}_{xx}^u & \mathbf{H}_{xy}^u & -\mathbf{G}_{xx}^u & -\mathbf{G}_{xy}^u \\ \mathbf{H}_{yx}^u & \mathbf{H}_{yy}^u & -\mathbf{G}_{yx}^u & -\mathbf{G}_{yy}^u \\ \mathbf{H}_{xx}^t & \mathbf{H}_{xy}^t & -\mathbf{G}_{xx}^t & -\mathbf{G}_{xy}^t \\ \mathbf{H}_{yx}^t & \mathbf{H}_{yy}^t & -\mathbf{G}_{yx}^t & -\mathbf{G}_{yy}^t \end{bmatrix} \quad \mathbf{f} = \begin{Bmatrix} \mathbf{f}_x^u \\ \mathbf{f}_y^u \\ \mathbf{f}_x^t \\ \mathbf{f}_y^t \end{Bmatrix} \quad \mathbf{x} = \begin{Bmatrix} \mathbf{u}_x \\ \mathbf{u}_y \\ \mathbf{t}_x \\ \mathbf{t}_y \end{Bmatrix}. \tag{48}$$

Solving the system (47) allows to obtain the coefficients u_{lj} and t_{lj} of the approximations $\tilde{u}_l^e$ and $\tilde{t}_l^e$. If the basis $\left\{N_j^e\right\}_{j=1}^{n_e}$ and $\left\{M_j^e\right\}_{j=1}^{m_e}$ adopted for the approximations $\tilde{u}_l^e$ and $\tilde{t}_l^e$ satisfy the Kronecker property at the anchor points (parametric coordinates of the collocation points), the coefficients u_{lj} and t_{lj} have the physical meaning of the fields u_l and t_l at those points. The displacements, strains and stresses solutions at interior points can be done in a post processing stage by using the integral equations for interior points (Beer *et al.*, 2020).

4. NUMERICAL RESULTS

4.1 Infinite plate with circular hole under constant in-plane tension

The first example deals with an infinite plate with a hole. The hole has a radius $R = 1$ m and the plate is subjected to a constant traction in x-direction $T_x = 10$ MPa at infinity. Due to the symmetry of the problem, only a finite quarter part of the domain is modeled, with side $L = 4$ m as shown in Figure 2a. The problem is in plane strain condition. The material properties used are $E = 100000$ MPa and $\nu = 0,3$. The analytical solution for stress, available in Barber (2002), can be presented as

$$\sigma_{rr}\,(r,\theta) = \frac{T_x}{2}\left(1 - \frac{R^2}{r^2}\right) + \frac{T_x}{2}\left(1 - 4\frac{R^2}{r^2} + 3\frac{R^4}{r^4}\right)\cos 2\theta \tag{48}$$

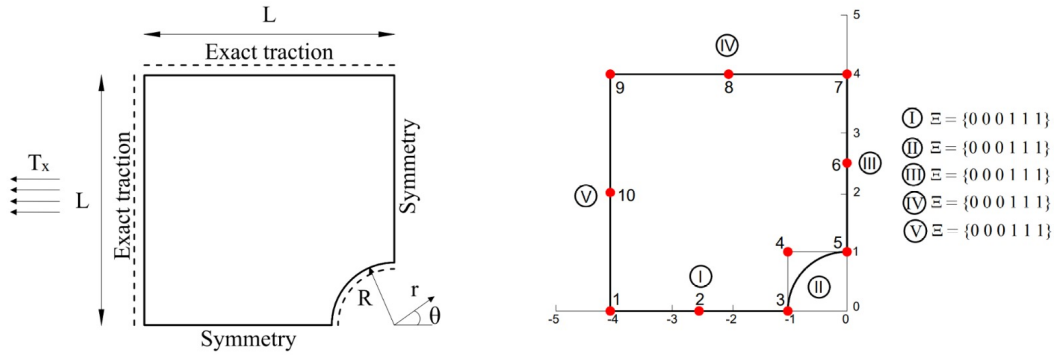

(a) Hole within a infinite plate (b) Control points and knot vectors

Figure 2. Hole within an infinite plate, problem and geometry definitions

$$\sigma_{\theta\theta}(r,\theta) = \frac{T_x}{2}\left(1+\frac{R^2}{r^2}\right) - \frac{T_x}{2}\left(1+3\frac{R^4}{r^4}\right)\cos 2\theta \tag{49}$$

$$\sigma_{\theta\theta}(r,\theta) = -\frac{T_x}{2}\left(1+2\frac{R^2}{r^2}-3\frac{R^4}{r^4}\right)\sin 2\theta \tag{50}$$

where r and θ are the coordinates of the polar system illustrated in Fig. 2a.

Five NURBS curves illustrated in Figure 2b are used to describe the boundary of the finite quarter part of the infinite plate. Notice that the exact traction conditions are prescribed on NURBS IV and V, where the infinite plate is cut. Thus, to obtain the exact traction boundary condition, it is necessary to apply the Cauchy balance $\mathbf{t} = \sigma\mathbf{n}$ to the analytical stress tensor $\sigma(x,y)$, written in Cartesian coordinates. The analytical stress tensor in Cartesian coordinates can be obtained from the analytical stress tensor in polar coordinates, using the rotation matrix. Zero traction boundary condition is prescribed on NURBS II, while symmetry conditions are prescribed on NURBS I and III.

Figure 3a presents the convergence results in terms of the L_2 norm of the traction error vector along the boundary for all refinement strategies studied. It can be observed that the best convergence results are obtained for the k-refinement, resulting an error of 10^{-5} for a basis of order 5. Notice that B-spline knot-insertion refinement resulted in convergence rates $p+1$ for B-splines of order p. Figure 3b illustrates the behavior p-refinement for Lagrange polynomial basis. The Runge's phenomenon is evident for high-order Lagrange polynomials. The worst B-spline convergence results, knot-insertion refinement with $p = 1$, is also illustrated in Figure 3b to emphasize the Runge's phenomenon problem. This highlights the advantage of using B-spline over a Lagrange polynomials.

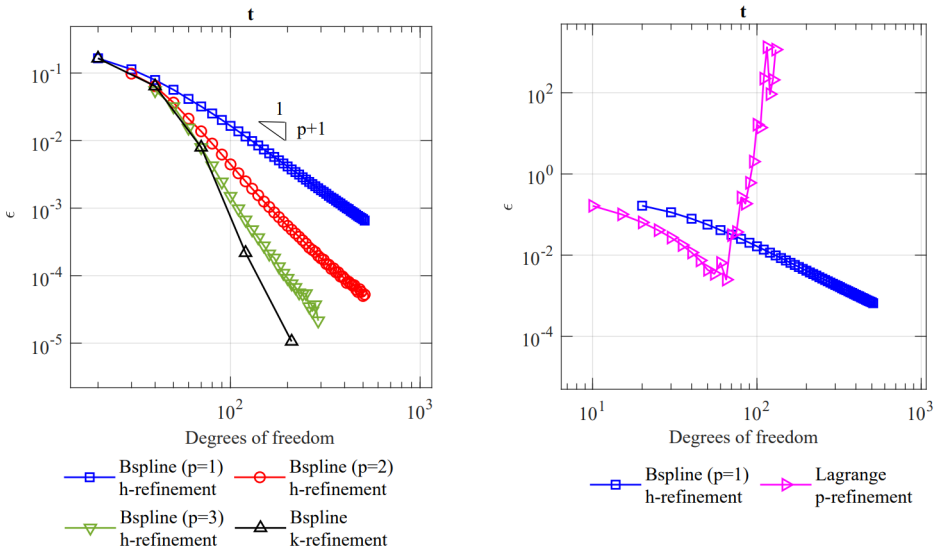

(a) Convergence error - h-refinement and k-refinement (b) Convergence error - Bspline and Lagrange

Figure 3. Convergence results in terms of the L_2 norm of the traction error vector along the boundary

4.2 Open spanner

The open spanner problem, presented as the last example and also found in Simpson *et al.* (2012), serves as an illustrative example for geometries arbitrary taken from CAD. The problem was modeled considering a plane strain condition and it is illustrated in Figure 4a. The spanner is subjected to bending by a uniform traction $t_y = -10$ MPa at the right edge. The material properties used are $E = 100000$ MPa and $\nu = 0.3$. The geometry definitions of the open spanner problem, i.e., control points and knot vectors, are shown in Figure 4b. Fixed boundary conditions are prescribed on NURBS I, II, and VI, while zero traction conditions is prescribed on NURBS III and V. NURBS IV is subjected to a uniform traction of $t_y = -10$ MPa and $t_x = 0$.

The analysis was performed using independent B-splines basis of order $p = 4$, defined over NURBS I-VI, for the boundary fields which resulted in a total of 400 collocation points. The post-processed internal stress field results are presented in Figure 4c in terms of Von Mises stresses. These results can be compared with those presented in Simpson *et al.* (2012), showing good agreement with the conventional IGABEM. The present example illustrates the possibility of performing analysis using arbitrary geometry information taken from CAD, with refined boundary field basis that did not interfered with the original CAD geometry.

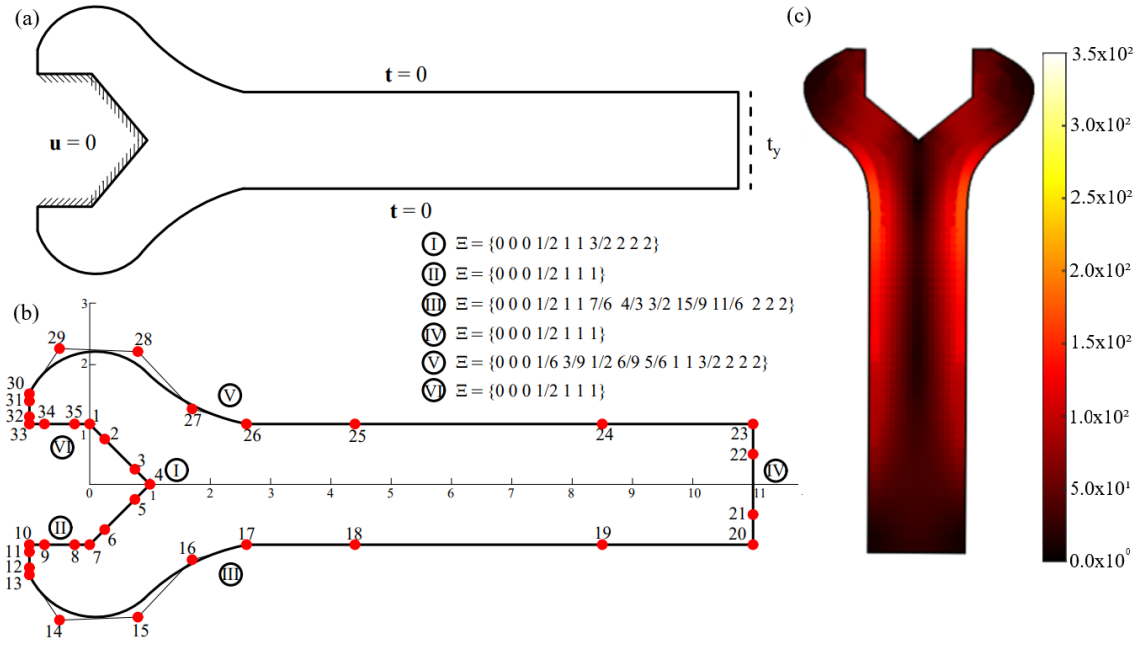

Figure 4. Open spanner geometry, control points, knot vector e Von Mises stress

5. CONCLUDING REMARKS

This work presented an improved independent basis IGABEM formulation. The main improvements are related to prescribing exact boundary conditions, resulting in a single matrix formulation, and using an auxiliary function to ensure continuity between prescribed and non-prescribed boundary displacements. The a single matrix approach reduces the memory storage requirements of the method. Prescribing exact boundary conditions without approximations can be highly beneficial in isogeometric analysis, especially when complex boundary conditions must be imposed. Moreover, boundary displacements continuity can be ensured by using the auxiliary function in the approximations. The independent basis approach allows refinement strategies without interfering with the geometrical model obtained from CAD. The results showed that Knot insertion presented convergence rates p+1 for B-splines of order p while p-refinement with Lagrange polynomials suffers with the Runge phenomenon. The superiority of B-splines k-refinement over the other refinement strategies was evident.

6. ACKNOWLEDGEMENTS

This work was funded by the Brazilian Coordination of Superior Level Staff Improvement (CAPES).

7. REFERENCES

Aliabadi, M., 2002. *The Boundary Element Method: Applications in Solids and Structures*. Chichester, Wiley.

Barber, J., 2002. *Elasticity*. Kluwer Academic Publishers.

Bazilevs, Y., Gohean, J., Hughes, T., Moser, R. and Zhang, Y., 2009. "Patient-specific isogeometric fluid–structure interaction analysis of thoracic aortic blood flow due to implantation of the jarvik 2000 left ventricular assist device". *Computer Methods in Applied Mechanics and Engineering*, pp. 3534–3550. URL https://doi.org/10.1016/j.cma.2009.04.015.

Beer, G. and Duenser, C., 2023. "Immersed isogeometric boundary elements: A user friendly method for the 3-d elasto-plastic simulation of underground excavations". *Computers and Geotechnics*, Vol. 157, p. 105330. URL https://doi.org/10.1016/j.compgeo.2023.105330.

Beer, G., Marussig, B. and Duenser, C., 2020. *The Isogeometric Boundary Element Method*. Springer. URL https://doi.org/10.1007/978-3-030-23339-6.

Cervera, E. and Trevelyan, J., 2005. "Evolutionary structural optimisation based on boundary representation of nurbs. part i: 2d algorithms". *Computers and Structures*, pp. 1902–1916. URL https://doi.org/10.1016/j.compstruc.2005.02.016.

Cottrell, J., Reali, A., Bazilevs, Y. and Hughes, T., 2006. "Isogeometric analysis of structural vibrations". *Computer Methods in Applied Mechanics and Engineering*, Vol. 195, No. -, pp. 5257–5296. URL https://doi.org/10.1016/j.cma.2005.09.027.

Cottrell, J.A., Hughes, T.J.R. and Bazilevs, Y., 2009. *Isogeometric Analysis: Toward Integration of CAD and FEA*. Wiley.

Cox, M., 1971. "The numerical evaluation of b-splines". *Journal of Applied Mathematics*, pp. 134–149. URL https://doi.org/10.1093/imamat/10.2.134.

DeBoor, C., 1972. "On calculation with b-splines". *Journal Approximation Theory*, Vol. 6, pp. 50–62. URL https://web.stanford.edu/class/cme324/classics/deboor.pdf.

Doz, J., Kurz, S., Schops, S. and Wolf, F., 2018. "A numerical comparison of an isogeometric and a classical higher-order approach to the electric field integral equation". *arXiv preprint arXiv:1807.03628*, Vol. -, No. -, pp. –. URL https://doi.org/10.48550/arXiv.1807.03628.

Hsiao, G., 2006. "Boundary element methods—an overview". *Applied Numerical Mathematics*, Vol. 56, No. 10-11, pp. 1356–1369. URL https://doi.org/10.1016/j.apnum.2006.03.030.

Hughes, T., Cottrell, J. and Bazilevs, Y., 2005. "Isogeometric analysis: Cad, finite elements, nurbs, exact geometry and mesh refinement". *Computer Methods in Applied Mechanics and Engineering*, Vol. 194, No. 39-41, pp. 4135–4195. URL https://doi.org/10.1016/j.cma.2004.10.008.

Lachat, J. and Watson, J., 1976. "Effective numerical treatment of boundary integral equations: A formulation for three-dimensional elastostatics". *International Journal for Numerical Methos in Engineering*, Vol. 10, No. -, pp. 91–1005. URL https://doi.org/10.1002/nme.1620100503.

Lipton, S., Evans, J., Y.Bazilevs, Elguedj, T. and Hughes, T., 2010. "Robustness of isogeometric structural discretizations under severe mesh distortion". *Computer Methods in Applied Mechanics and Engineering*, pp. 357–373. URL https://doi.org/10.1016/j.cma.2009.01.022.

Liu, Z., Majeed, M., Cirak, F. and Simpson, R., 2017. "Isogeometric fem-bem coupled structural-acoustic analysis of shells using subdivision surfaces". *International Journal for Numerical Methods in Engineering*, Vol. 113, No. 9, pp. 1507–1530. URL https://doi.org/10.1002/nme.5708.

Marussig, B., 2015. *Seamless Integration of Design and Analysis through Boundary Integral Equations*. Ph.D. thesis, Graz University of Technology, Graz, Austria.

Marussig, B., Zechner, J., Beer, G. and T.Fries, 2015. "Fast isogeometric boundary element method based on independent field approximation". *Computer Methods in Applied Mechanics and Engineering*, Vol. 284, No. 1, pp. 458–488. URL https://doi.org/10.1016/j.cma.2014.09.035.

Peng, X., Atroshchenko, E., Kerfriden, P. and Bordas, S., 2017. "Linear elastic fracture simulation directly from cad: 2d nurbs-based implementation and role of tip enrichment". *International Journal of Fracture*, Vol. 204, pp. 55–78. URL https://doi.org/10.1007/s10704-016-0153-3.

Piegl, L. and Tiller, W., 1995. *The NURBS book*. Springer.

Simpson, R., Bordas, S., Trevelyan, J. and Rabczuk, T., 2012. "A two-dimensional isogeometric boundary element method for elastostatic analysis". *Applied Mathematical Modeling*, Vol. 209, No. 212, pp. 87–100. URL https://doi.org/10.1016/j.cma.2011.08.008.

Simpson, R., Scott, M., Taus, M., Thomas, D. and Lian, H., 2014. "Acoustic isogeometric boundary element analysis". *Computer Methods in Applied Mechanics and Engineering*, Vol. 269, No. 1, pp. 265–290. URL https://doi.org/10.1016/j.cma.2013.10.026.

8. RESPONSIBILITY NOTICE

The authors Guilherme Henrique Teixeira, Francisco Alex Correia Monteiro and Sérgio Gustavo Ferreira Cordeiro are solely responsible for the printed material included in this paper.